Lab on a Chip

Accepted Manuscript

ROYAL SOCIETY OF CHEMISTRY

www.rsc.org/loc

Abstract: We report a smartphone spectrometer with nanometer resolution working in the visible range. A G-Fresnel device with the dual functionality of focusing and dispersion is used to enable miniaturization. Proof of principle application to Bradford assay of protein concentration is also demonstrated.

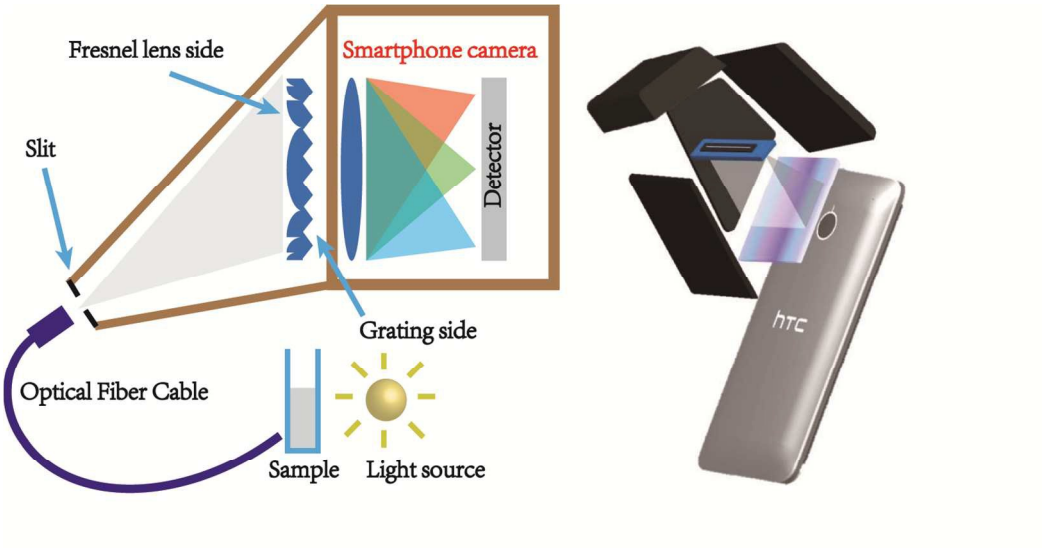

Lab on a Chip

COMMUNICATION

G-Fresnel smartphone spectrometer

Chenji Zhang,[a] Gong Cheng,[b] Perry Edwards,[a] Ming-Da Zhou,[b] Siyang Zheng[b] and Zhiwen Liu*[a]

Received 00th January 20xx,
Accepted 00th January 20xx

DOI: 10.1039/x0xx00000x

www.rsc.org/

We report a smartphone spectrometer with nanometer resolution working in the visible range. A G-Fresnel device with the dual functionality of focusing and dispersion is used to enable miniaturization. Proof of principle application to Bradford assay of protein concentration is also demonstrated.

As of 2013, there were over 6.8 billion mobile phones in the world, approaching the total population on Earth (~7 billion)[1]. The emergence of smartphones, in just a few years, has fundamentally changed our perception of a cell phone as a basic communication tool. As the mobile computing hardware continues to get faster and more powerful, there is a growing interest to develop new devices that can augment the capability of a smartphone to expand its applications, in particular, to sensing, while fully exploiting the communicational and computational power of modern smartphones. One of the key enabling technologies for sensing is optical spectroscopy, which can provide quantitative information of chemical species by interrogating the interaction between light and matter and has found numerous applications in biological and biomedical instrumentation and research[2–8]. As such, in recent years much effort has been devoted to developing compact optical spectrometers. Existing work includes micro-fabricated devices[9–14], the use of curved gratings[1516], and filter based miniature spectrometers[17–20]. Efforts to integrate spectrometers with cell phones are also underway[2-5]. By directly using the built-in camera and a transmission grating, a smartphone spectrometer with a resolution down to 5 nm was developed in 2011[21]. A MEMS device was designed to replace the grating, which has proven efficient due to the capability to integrate multiple optical elements[22]. Also, a smartphone spectrometer based on a reflection grating was reported, which had an integrated light source and was capable of both absorption and fluorescence measurements[23]. Moreover, Smartphone spectrometers have already found promising applications to fluorescence measurement, enzyme-linked immunosorbent assay, and label-free biodetection[24–26]. Despite the significant progress, how to further reduce the size and cost while maintaining the performance of smartphone spectrometers remains a challenge.

Here we present a smartphone spectrometer by using a dual-functionality diffractive optical element, G-Fresnel[27,28], which can simultaneously focus and disperse an impinging light. Note that the performance of a traditional grating based dispersive spectrometer can be described by a system metric *E*, the product of the resolving power (λ/Δλ) and the system etendue[29]:

$$E \propto \frac{\lambda V^{2/3}}{\Lambda \left(F/\#\right)^{5/3}} \qquad (1).$$

Here λ is the wavelength, Δλ is the wavelength resolution, Λ is the grating period, *V* is the volume of the spectrometer, and *F/#* is the ratio between the focal length and aperture size of the system. Thus, the higher the resolving power and the system throughput (hence measurement sensitivity), the higher *E* is. Clearly, a large *E* implies a large *V*, which is the dilemma for developing a high-performance miniature spectrometer. The G-Fresnel can realize wavelength dispersion and light focusing as well as collimation in a single device, and can thus replace multiple discrete optical components in a traditional spectrometer to result in a more compact design (hence a much smaller *V*), without compromising the performance metric *E*. The G-Fresnel can also have a small *F#* which can greatly decrease the size of the spectrometer while improving the system performance (cf. Eq. 1). In addition, the G-Fresnel can be fabricated by using surface molding method, which is cost-efficient and has the potential for low-cost mass production.

[a] Department of Electrical Engineering, The Pennsylvania State University, University Park, Pennsylvania 16802, U.S.A.
[b] Department of Biomedical Engineering and Materials Research Institute, The Pennsylvania State University, University Park, PA 16802, U.S.A. .
†Electronic Supplementary Information (ESI) available: See
DOI: 10.1039/x0xx00000x

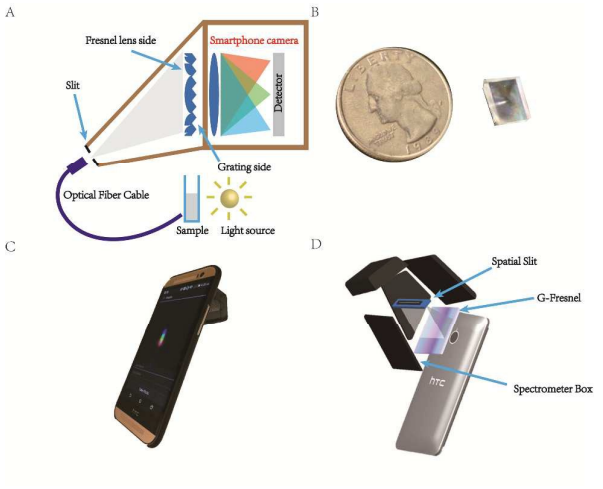

Figure 1 G-Fresnel smartphone spectrometer (a) Schematic diagram of the G-Fresnel smartphone spectrometer (b) a photo of a transmission G-Fresnel device compared to a US quarter dollar coin (c) a prototype G-Fresnel smartphone spectrometer (d) Schematic depicting the assembly of the prototype

The functionality of G-Fresnel was previously demonstrated in a bench-top spectrometer system[28]. Here, it is used for realization of a smartphone spectrometer. The schematic is shown in Figure 1a. The smartphone used in our experiments is an HTC One (M8) with Android OS, v4.4.2. The G-Fresnel is placed directly in front of the smartphone camera with the grating side facing in. A photo of a G-Fresnel is shown in Figure 1b. The detailed working principle and fabrication process of G-Fresnel was described in Ref. [27] (schematic diagrams of the fabrication procedure are provided in Figure S1 in the supplementary material). Briefly, PDMS (Dow Corning Sylgard 184 Silicone) pre-polymer is poured onto the surface of a Fresnel lens (Edmund Optics 2.0" x 2.0", 1.0" FL, Aspheric Fresnel Lens). After baking the PDMS for 12hours at 60 °C, the PDMS is cured completely and a negative Fresnel lens mold is obtained. The same method is used to fabricate a negative mold of a diffraction grating (Thorlabs Vis Trans Grating, 1200 Grooves/mm, 36.9° Blaze Angle, 12.7 mm x 12.7 mm). A G-Fresnel can be fabricated by sandwiching PDMS pre-polymer between the grating and the negative Fresnel lens molds (with minimum alignment requirement) followed by curing. As shown by Figure 1a, light emanating from the entrance slit is collimated by the Fresnel lens side of the G-Fresnel and dispersed by the grating side. Different wavelengths are thus focused by the camera lens onto different positions on the imaging sensor. It should be noted that in principle the smartphone camera lens is not necessary and the entire collimation, focusing, and dispersion functionality can be realized using a single G-Fresnel as previously shown in Ref. [28]. The G-Fresnel thus significantly reduces the size of the spectrometer. The spectrometer system shown in Figure 1 c and d has a dimension of 1.8” x 0.8” x 0.9”. The prototype enclosure was fabricated using a 3D printer. Slots are designed to hold the G-Fresnel and the slit at pre-aligned positions. The device was then secured to a smartphone case, which could be attached to the smartphone as a single accessory. Due to the compact and stable design, the shift caused by removing and re-installing the prototype attachment is within 10 pixels (corresponding to 3-4 nm wavelength shift), which can be neglected for many applications and recalibrated easily if necessary. Additionally, the system is designed to use either an optical fiber or free space for light delivery.

The calibration of the spectrometer is divided into two steps, i.e., wavelength calibration and intensity calibration. A mercury and argon calibration source (Ocean optics HG-1 Mercury Argon Calibration Source) that has several emission lines in the visible range was used for wavelength calibration. A typical spectrum is shown in Figure 2a. By comparing the spectrum with the emission wavelengths of the calibration source, the pixel-wavelength relationship can be obtained as plotted in Figure 2b. The linear relationship enables easy calibration for the device. To perform the intensity calibration, we compared the measurements of a common optical signal obtained by using the G-Fresnel smartphone spectrometer and a commercial spectrometer. To this end, a fiber probe (Ocean Optics R400-7-SR) consisting 6 surrounding fibers for light delivery and a central fiber for light collection was placed above an optical diffuser (Ocean Optics WS-1 Reflectance Standards). The diffuse reflectance spectrum was measured by using the G-Fresnel spectrometer and an Ocean Optics USB4000 spectrometer, respectively. Let us denote the reference spectrum (measured by the Ocean Optics spectrometer) as I(λ). Note that colored imaging sensors used by today’s smartphones are usually Bayer sensors, which are 2D arrays of detector pixels with red, green and blue color filters arranged in a Bayer pattern. The red, green and blue filter response function r(λ), g(λ) and b(λ) can be calibrated by comparing the measurement result R(λ), G(λ) and B(λ) (i.e., the red, green, and blue pixel values) from the smartphone spectrometer with I(λ): $R(\lambda) = r(\lambda)I(\lambda), G(\lambda) = g(\lambda)I(\lambda), B(\lambda) = b(\lambda)I(\lambda)$. When another spectral measurement is made, results R’(λ), G’(λ) and B’(λ) from the smartphone spectrometer can be converted to a calibrated spectrum I’(λ) in the least square sense: $I'(\lambda) = \frac{r(\lambda)R'(\lambda)+g(\lambda)G'(\lambda)+b(\lambda)B'(\lambda)}{r(\lambda)^2+g(\lambda)^2+b(\lambda)^2}$. It should be pointed out that both the focusing (at infinity) and white balance of the smartphone camera need to be fixed in order to ensure calibration and measurement consistency.

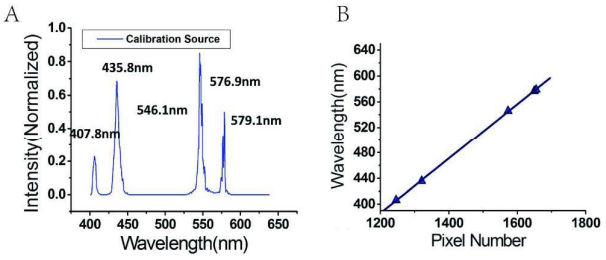

Figure 2 Wavelength calibration (a) Measured spectrum of a mercury argon calibration source (b) Linear relationship between the pixel number and the calibrated wavelength

However, due to the built-in sophisticate post image-processing in smartphones, the retrieved spectra may still suffer from these artifacts. A better approach is to directly use the raw data from the smartphone camera, which is free from image processing. We note that some recent Android based smartphones have started to offer this capability (e.g., HTC one M9).

The spectral resolution was experimentally studied by using spectral holography. A supercontinuum source generated by propagating a 1064 nm pulsed laser (JDS Uniphase NanolaseTM NP-10620-100 laser) in a 20-meter long nonlinear photonic crystal fiber (Blaze Photonics SC-5.0-1040) was directed to a Michelson interferometer (Figure S2 in the supplementary material). The slight optical path length difference between the two arms of the Michelson interferometer resulted in a spectral interference pattern as shown in Figure 3a measured by using the G-Fresnel smartphone spectrometer. The interference pattern was clearly resolved by the G-Fresnel spectrometer, yielding a spectral resolution of ~ 1.6 nm at 595 nm. The spectral holography measurement also demonstrated the viability of applying the G-Fresnel spectrometer to coherence measurement.

The theoretical spectral resolution of the device was also calculated as shown in Figure 3b. A geometric ray tracing method was used to estimate the image size $D(\lambda)$ of the slit (5μm width) on the smartphone CMOS sensor. The spectral resolution, defined as the wavelength difference such that the slit images at two wavelengths are separated by $D(\lambda)$, can be obtained by $\Delta\lambda = \frac{D(\lambda)}{F\frac{\partial\theta}{\partial\lambda}}$, where F is the focal length of the smartphone camera lens and $\frac{\partial\theta}{\partial\lambda}$ is the angular dispersion of the G-Fresnel. Our calculation also took into account of the wavelength dependent focal length of the G-Fresnel. To mitigate this chromatic aberration, the detector may be tilted as discussed previously[27]. As shown in Figure 3b, a resolution of 1.3 nm to 2.1 nm can be potentially achieved across the wavelength measurement range of 400 nm-650 nm, where the long wavelength is limited by the built-in infrared filter in the smartphone camera. We note that the spectral resolution at the long wavelength end agrees well with the calculated result, but that at the short wavelength end (full width at half maximum ~ 5nm near 400 nm,

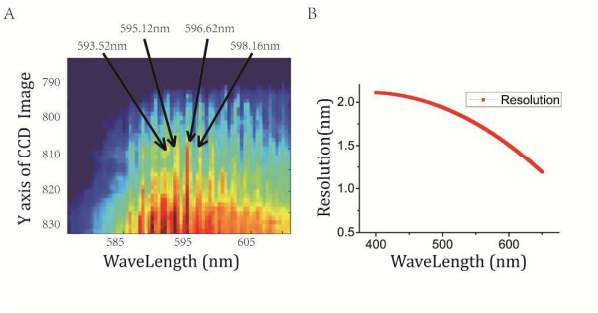

Figure 3 (a) Spectral holography characterization (b) Calculated spectral resolution

Fig. 2a) is worse than the theoretical estimate, which is likely due to non-optimized system alignment and possible performance degradation of the Fresnel side at shorter wavelengths.

One promising application of the G-Fresnel smartphone spectrometer is its ability to perform quantitative colorimetric analysis and thus provide a portable platform for chemical assay. In particular, determining the concentration of proteins in solutions is an important and regular step in many laboratory workflows that involve protein extraction and analysis in biological research, biomedical assay, food science, biocatalytic industry and environmental monitoring[30–34]. Optical spectrometer based colorimetric assays are among the most widely used strategies[35,36]. These methods are effective with the use of conventional bulky spectrometers in laboratories; however, as proteins are intrinsically prone to perish without preservation, limitations of these methods are apparent, especially for increasing requirements of immediate processing and detection of protein samples out of laboratory. The portable smartphone spectrometer thus shows a great advantage to address these issues. Bradford assay, as a typical colorimetric protein assay, is a fast and one of the most widely used spectroscopic analytical procedure. It analyzes the red shift of the absorbance spectrum of a reagent solution when binding to protein occurs[37,38].

A sample holder (1" × 1" × 2") was fabricated by using a 3D printer (Figure S3-a in the supplementary material). Standard polystyrene cuvettes containing a specimen solution can be placed inside. The sample holder also has two pre-aligned through-holes, which are used to attach a source fiber that is connected to a tungsten halogen light source (HL-2000-HP) and a detection fiber that couples the transmitted light to the G-Fresnel spectrometer. It is worth mentioning that an optical fiber can potentially be used to direct the built-in smartphone flashlight to a sample, or alternatively, the tungsten halogen light source may be replaced with a white LED. The transmission spectrum of specimen is normalized against a reference spectrum (i.e., transmission spectrum of the solvent, e.g. water) to obtain the absorbance $A=-\log_{10}\left(T_{specimen}/T_{water}\right)$. To characterize the system linearity, the absorbance spectrums of Rhodamine 6G (R6G) dye solutions with concentrations of 1μM, 2μM, 4μM, 6μM, 8μM, and 10μM were measured (Figure S3 and S4 in the supplementary material). By plotting the absorbance at two exemplary wavelengths (480nm, 524nm) as a function of concentration, the linear regression curves have R^2 values of 0.9995 (524 nm) and 0.9971 (480 nm) respectively, indicating an excellent linear response of the device ideally suitable for performing quantitative concentration measurement (Figure S4). To demonstrate the proof of concept for protein concentration measurement, standard Bradford reagent (SIGMA-ALDRICH B6916, Linear concentration range: 0.1–1.4 mg/ml) was used to measure

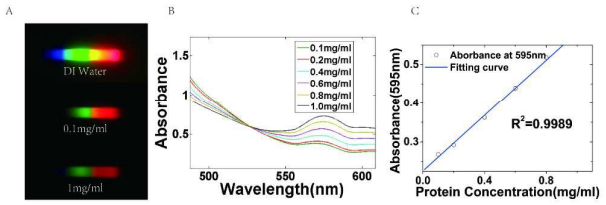

Figure 4 (a) Transmission spectrum images for DI water, Bradford reagent with 0.1mg/ml and 1mg/ml BSA (b) Absorbance spectra of Bradford reagent with different concentrations of BSA (d) Linear relation between the BSA concentration and the absorbance at 595nm

the concentration of bovine serum albumin (BSA). Initially, 0.01ml, 0.02ml, 0.04ml, 0.06ml, 0.08ml, 0.1ml BSA solution with a density of 0.1mg/ml was added into cuvettes. Then all the cuvettes were filled to 0.1ml with de-ionized water (DI water). After that, 5ml Bradford reagent was added to each cuvette. After mixing and resting the solutions for 10 minutes, the transmission spectrums were measured by the smartphone spectrometer. The captured spectrum images of DI water and Bradford reagent with 0.1mg/ml and 1mg/ml BSA are shown in Figure 4a. The absorption of the blue part of the spectrum can be clearly observed. A series of spectra with the BSA concentrations varied from 0.1 mg/ml to 1 mg/ml are shown in Figure 4b. There clearly exists an isosbestic point near 525nm and the absorbance across the isosbestic point exhibit opposite correlation to the protein concentration. In other words, as the BSA concentration increases the absorbance spectrum experiences a red shift and an absorbance peak appears at around 580 nm (expected to be 595nm). The wavelength discrepancy is mainly attributed to detector's RGB filter response. The green and red band edge causes the apparent dramatic increase in absorbance at 580nm as also previously noted[39]. Nevertheless, this error does not seem to affect the concentration measurement. We plotted the absorbance at 595nm as a function of the concentration of BSA (Figure 4c) and obtained a linear relation with R^2=0.998, demonstrating the capability of our smartphone spectrometer for quantitative measurement of protein concentration. It should be noted that in this study the sensitivity is primarily limited by the Bradford assay itself. With the rapid development of biotechnology, increasingly colorimetric methods and reagents with high sensitivity have been reported[40–42]. Our G-Fresnel smartphone spectrometer can also serve as a platform for these assays with high sensitivity.

Conclusions

We developed a compact (1.8" x 0.8" x 0.9") smartphone optical spectrometer in the visible wavelength range by using a G-Fresnel diffractive optical element. The wavelength-pixel mapping relationship was calibrated by using a mercury and argon calibration source with discrete emission lines. The intensity of the spectrometer was calibrated against a commercial optical spectrometer. We also demonstrated spectral holographic measurement by using the G-Fresnel smartphone spectrometer and carried out theoretical analysis of the spectral resolution, which indicated that the system could achieve a wavelength resolution of few nanometers. Several factors, including the grating groove density, chromatic aberration and performance of G-Fresnel, and slit size, limit the resolution of our G-Fresnel spectrometer. By optimizing the fabrication of G-Fresnel and its performance at the shorter wavelengths as well as compensating for the chromatic dispersion using a tilted detector array, spectral resolution of 1 nm can be potentially achieved as indicated by previous theoretical analysis[28]. A key innovation of our smartphone spectrometer is the use of the G-Fresnel device. It combines the functions of collimation, dispersion and collection in a single thin-film element. It can have a low f-number, leading to a compact system. Further, it may be realized by surface relief patterning, opening the possibility of low-cost volume production through replicating from a master pattern. The G-Fresnel thus opens a promising new avenue towards spectrometer miniaturization. We also demonstrated smartphone based Bradford assay, a powerful method for determining protein concentrations crucial for a variety of applications ranging from disease diagnosis to fundamental biomedical research. We performed proof-of-concept measurement of the BSA concentration. As the concentration of BSA increased, an absorption redshift was observed. A superb linear relationship between the absorbance and the protein concentration with R^2 > 0.99 was demonstrated. Notably, as we provide a general strategy for portable and convenient quantitative colorimetric analysis, it is expected that this platform can also be extended to other spectroscopic applications, such as, for food safety and medical care.

Acknowledgement

This work is supported by Vodafone Americas Foundation.

Conflict of interest

ZL and PE have a financial interest in Atoptix LLC, a company which could potentially benefit from the results of this research. This interest has been reviewed by the University in accordance with its Individual Conflict of Interest policy, for the purpose of maintaining the objectivity and the integrity of research at The Pennsylvania State University.

References

1 B. Sanou, *World 2013ict facts Fig.*, 2013.
2 L. Zhao, T. Wu, J.-P. Lefèvre, I. Leray and J. A. Delaire, *Lab Chip*, 2009, **9**, 2818–23.
3 J. Sun, Y. Xianyu and X. Jiang, *Chem. Soc. Rev.*, 2014, **43**, 6239–53.
4 E. Chung, R. Gao, J. Ko, N. Choi, D. W. Lim, E. K. Lee, S.-I. Chang and J. Choo, *Lab Chip*, 2013, **13**, 260–6.
5 C. H. Liu, B. B. Das, W. L. Sha Glassman, G. C. Tang, K. M. Yoo, H. R. Zhu, D. L. Akins, S. S. Lubicz, J. Cleary and R. Prudente, *J. Photochem. Photobiol. B.*, 1992, **16**, 187–209.

6 R. Richards-Kortum and E. Sevick-Muraca, *Annu. Rev. Phys. Chem.*, 1996, **47**, 555–606.
7 K. Sokolov, M. Follen and R. Richards-Kortum, *Curr. Opin. Chem. Biol.*, 2002, **6**, 651–658.
8 C. Krafft and V. Sergo, *Spectroscopy*, 2006, **20**, 195–218.
9 K. Chaganti, I. Salakhutdinov, I. Avrutsky and G. W. Auner, *Opt. Express*, 2006, **14**, 4064–4072.
10 R. F. Wolffenbuttel, *J. Micromechanics Microengineering*, 2005, **15**, S145.
11 X. Gan, N. Pervez, I. Kymissis, F. Hatami and D. Englund, *Appl. Phys. Lett.*, 2012, **100**.
12 E. Laux, C. Genet, T. Skauli and T. W. Ebbesen, *Nat. Photonics*, 2008, **2**, 161–164.
13 D. Knipp, H. Stiebig, S. R. Bhalotra, S. Member, E. Bunte, H. L. Kung, S. Member and D. A. B. Miller, 2005, **52**, 419–426.
14 B. Redding, S. F. Liew, R. Sarma and H. Cao, *Nat. Photonics*, 2013, **7**, 746–751.
15 Http://www.hamamatsu.com/jp/en/C12666MA.html, .
16 C. A. Palmer, E. G. Loewen and R. G. L. Thermo, *Diffraction grating handbook*, Newport Corporation Springfield, Ohio, USA, 2005.
17 S.-W. Wang, C. Xia, X. Chen, W. Lu, M. Li, H. Wang, W. Zheng and T. Zhang, *Opt. Lett.*, 2007, **32**, 632–634.
18 A. Emadi, H. Wu, G. de Graaf and R. Wolffenbuttel, *Opt. Express*, 2012, **20**, 489.
19 J. Bao and M. G. Bawendi, 2013.
20 U. Kurokawa, B. Il Choi and C. C. Chang, *IEEE Sens. J.*, 2011, **11**, 1556–1563.
21 Z. J. Smith, K. Chu, A. R. Espenson, M. Rahimzadeh, A. Gryshuk, M. Molinaro, D. M. Dwyre, S. Lane, D. Matthews and S. Wachsmann-Hogiu, *PLoS One*, 2011, **6**.
22 A. Das, T. Swedish, A. Wahi, M. Moufarrej, M. Noland, T. Gurry, E. Aranda-Michel, D. Aksel, S. Wagh and V. Sadashivaiah, in *SPIE Sensing Technology+ Applications*, International Society for Optics and Photonics, 2015, p. 94820M–94820M.
23 M. Arafat Hossain, J. Canning, S. Ast, K. Cook, P. J. Rutledge and A. Jamalipour, *Opt. Lett.*, 2015, **40**, 1737–1740.
24 K. D. Long, H. Yu and B. T. Cunningham, *Biomed. Opt. Express*, 2014, **5**, 3792–3806.
25 D. Gallegos, K. D. Long, H. Yu, P. P. Clark, Y. Lin, S. George, P. Nath and B. T. Cunningham, *Lab Chip*, 2013, **13**, 2124–32.
26 K. D. Long, H. Yu and B. T. Cunningham, in *SPIE Sensing Technology+ Applications*, International Society for Optics and Photonics, 2015, p. 94820J–94820J.
27 C. Yang, K. Shi, P. Edwards and Z. Liu, *Opt. Express*, 2010, **18**, 23529–23534.
28 C. Yang, P. Edwards, K. Shi and Z. Liu, *Opt. Lett.*, 2011, **36**, 2023–2025.
29 D. J. Brady, *Optical imaging and spectroscopy*, John Wiley & Sons, 2009.
30 I. de Andrade Brito, C. A. Freire, F. Y. Yamamoto, H. C. S. de Assis, L. R. Souza-Bastos, M. M. Cestari, N. de Castilhos Ghisi, V. Prodocimo, F. F. Neto and C. A. de Oliveira Ribeiro, *J. Environ. Monit.*, 2012, **14**, 615–625.
31 J. Ge, J. Lei and R. N. Zare, *Nat. Nanotechnol.*, 2012, **7**, 428–432.
32 Y. Hanada, K. Sugioka and K. Midorikawa, *Lab Chip*, 2012, **12**, 3688–3693.
33 A. M. Koskey, J. C. Fisher, M. F. Traudt, R. J. Newton and S. L. McLellan, *Appl. Environ. Microbiol.*, 2014, **80**, 757–765.
34 P. R. Salgado, M. E. López-Caballero, M. C. Gómez-Guillén, A. N. Mauri and M. P. Montero, *Food Hydrocoll.*, 2013, **33**, 74–84.
35 M. A. Redmile-Gordon, E. Armenise, R. P. White, P. R. Hirsch and K. W. T. Goulding, *Soil Biol. Biochem.*, 2013, **67**, 166–173.
36 J. P. D. Goldring, *West. Blotting Methods Protoc.*, 2015, 41–47.
37 M. M. Bradford, *Anal. Biochem.*, 1976, **72**, 248–254.
38 S. J. Compton and C. G. Jones, *Anal. Biochem.*, 1985, **151**, 369–374.
39 H. Yu, Y. Tan and B. T. Cunningham, *Anal. Chem.*, 2014.
40 J.-J. Feng, H. Guo, Y.-F. Li, Y.-H. Wang, W.-Y. Chen and A.-J. Wang, *ACS Appl. Mater. Interfaces*, 2013, **5**, 1226–1231.
41 D. Vilela, M. C. González and A. Escarpa, *Anal. Chim. Acta*, 2012, **751**, 24–43.
42 P. Miao, T. Liu, X. Li, L. Ning, J. Yin and K. Han, *Biosens. Bioelectron.*, 2013, **49**, 20–24.